

# Highly Efficient Polymeric Electrophosphorescent Diodes\*\*

By Xiaohui Yang, David C. Müller, Dieter Neher,\* and Klaus Meerholz\*

Intense research activities have been stimulated since Tang et al.<sup>[1]</sup> and Friend and co-workers<sup>[2]</sup> demonstrated efficient organic light-emitting diodes (OLEDs) based on small molecules (SMs) and polymers. In the past, significant progress has been made towards higher efficiencies and longer lifetimes by using more intelligent device structures and improved organic semiconductors. Previously, the world of OLEDs was dominated by fluorescent emitters. In 1998, Baldo et al.<sup>[3]</sup> demonstrated efficient OLEDs based on phosphorescent emitters to overcome the efficiency limit imposed by the formation of singlet excitons (25 %). This concept yielded highly efficient electrophosphorescent devices with emission colors across the entire visible spectral region,<sup>[3–10]</sup> most of them based on carbazole-containing hosts such as 4,4'-bis(*N*-carbazolyl) biphenyl (CBP).

Stimulated by this success, research activities have also been directed to polymer electrophosphorescent devices.<sup>[11–21]</sup> Recent work by Neher and co-workers on electrophosphorescent devices based on poly(vinylcarbazole) (PVK) doped with the electron-transporting molecule 2-(4-biphenyl)-5-(4-*tert*-butylphenyl)-1,3,4-oxadiazole (PBD) and a very soluble derivative of Ir(ppy)<sub>3</sub> (where ppy = phenylpyridine) suggested that charge injection imposes a severe limit on brightness and efficiency.<sup>[16]</sup> A significant improvement was achieved by using CsF/Al or Cs/Al as the cathode.<sup>[15–18]</sup> It was further possible to improve hole injection from the polymeric PEDOT:PSS [poly(3,4-ethylenedioxythiophene) doped with poly(styrene sulfonate)] anode by adding the well-known hole-transporting molecule *N,N'*-diphenyl-*N,N'*-(bis(3-methylphenyl)-[1,1-biphenyl]-4,4'-diamine (TPD) to the PVK-based emission layer.<sup>[18]</sup> Electrophosphorescent devices with an optimized layer composition exhibited a maximum external quantum

efficiency (EQE) of 10.7 %. More recently, Suzuki et al. demonstrated a maximum EQE of 11.8 % and a power efficiency (PE) of 38.6 lm W<sup>-1</sup> in a device using a copolymer bearing TPD, PBD, and a green-light-emitting phosphor as side groups.<sup>[21]</sup> Up to now, these are the most efficient polymeric electrophosphorescent green-light-emitting devices.

Despite recent improvements, the efficiencies of polymer electrophosphorescent devices are still inferior to their respective SM counterparts.<sup>[3–10]</sup> A plausible reason for this might be the necessity to realize a complex multilayer device architecture to achieve ultrahigh efficiencies. This is inherently much more difficult for the solution-processing technique that is commonly used for polymeric light-emitting devices. In fact, highly efficient diodes (with efficiencies up to 11 and 55 cd A<sup>-1</sup> for red- and green-light emission, respectively), comprising a solution-processed emission layer and an evaporated electron-transporting/hole-blocking layer, have been produced recently.<sup>[20,22]</sup> The most promising approach to achieve multiple layers for purely solution-processed devices is the conversion of a soluble precursor to an insoluble polymer film by polymerizing reactive side groups, allowing the sequential deposition of, in principle, an unlimited number of layers. There are only a few examples of this approach, and the most successfully used systems contain oxetanes as the reactive units, which can be reacted cationically. For example, a variety of triarylamine-based hole-conducting materials were used as graded hole-injection layers to build highly efficient polymer blue-light-emitting diodes.<sup>[23]</sup> Later, poly-spirofluorene copolymers functionalized with these crosslinkable moieties were demonstrated to work as negative photoresists, allowing the fabrication of laterally structured multicolored (red-green-blue) RGB polymer light-emitting diodes.<sup>[24]</sup> Note that several reports exist about polymer electrofluorescent and electrophosphorescent devices based on crosslinkable hole-transporting layers, but the efficiencies of these devices without an evaporated electron-transporting/hole-blocking layer are only moderate.<sup>[25,26]</sup>

As mentioned above, highly efficient polymer electrophosphorescent devices have been realized previously with a polymer blend consisting of PVK/PBD (in a weight ratio 71:29) as the host doped with the green-light-emitting phosphorescent dye tris(2-(4-tolyl)phenylpyridine)iridium [Ir(mppy)<sub>3</sub>] (see Fig. 1). In these devices, which have PEDOT:PSS anodes, an Ir(mppy)<sub>3</sub> concentration of 0.7 wt % has been found to be optimum.<sup>[16]</sup> This device structure is used here as a reference and referred to as G-X0-0.7 (the rule for the nomenclature being “color-*Xn*-dye content”, where the color can be red, green, or blue, and *n* is the number of crosslinked layers).

[\*] Prof. K. Meerholz, Dr. D. C. Müller  
University of Cologne, Institute of Physical Chemistry  
Luxemburgerstr. 116, 50939 Köln (Germany)  
E-mail: klaus.meerholz@uni-koeln.de

Prof. D. Neher, Dr. X. Yang  
University of Potsdam, Institute of Physics  
Am Neuen Palais 10, 14469 Potsdam (Germany)  
E-mail: Dieter.Neher@physik.uni-potsdam.de

[\*\*] This work was supported by the Bundesministerium für Bildung und Forschung (BMBF, Germany) through grant 13N8213. We acknowledge experimental support by N. Riegel, A. Köhnen, Dr. R. Alle, and P. Zacharias from the University of Cologne. We also express our thanks to Prof. O. Nuyken (TU Munich, Germany) and his group for fruitful discussions.

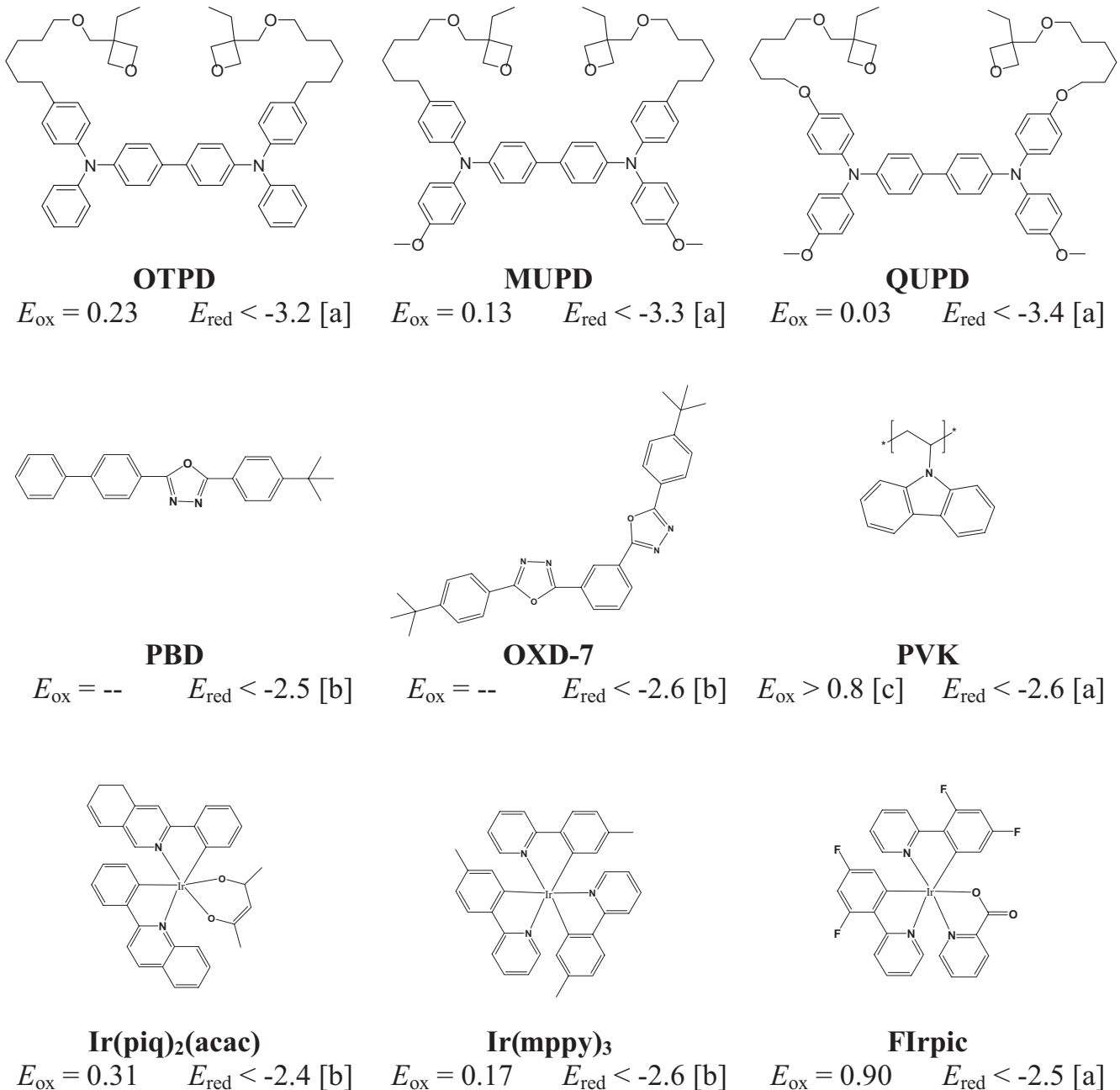


**Figure 1.** Chemical structures and redox potentials ( $E_{\text{ox,red}}$ ) of the compounds used in this study. The redox potentials were measured in dichloromethane (0.1 M tetrabutylammonium hexafluorophosphate) and calibrated versus the ferrocene/ferrocenium redox couple. [a] Estimated from the oxidation potential and the optical gap. [b] Chemically irreversible (multiple electron transfer). [c] Chemically irreversible (dimer formation).

It was found in previous investigations that hole injection is the limiting step in these devices. Therefore, to facilitate hole injection, we first studied devices with a single crosslinked hole-transporting layer (X-HTL). The selection of the proper hole conductor was guided by the criteria that its highest occupied molecular orbital (HOMO) level should be located between the work function of the PEDOT:PSS anode and that of the emitting dopant (or polymer host). Therefore, MUPD and OTPD were tested, as these ideally fulfill this condition

(see Fig. 1). No significant difference in device performance using either MUPD or OTPD as the hole conductor was observed. We attribute this to the fact that the offset between the X-HTL HOMO and the HOMO of the emitter is very small. For the following investigations we restricted ourselves to MUPD.

Figure 2a shows the current-density–brightness–voltage ( $J$ – $L$ – $V$ ) characteristics of the devices with an Ir(mppy)<sub>3</sub> concentration of 0.7 wt % and a single crosslinked MUPD hole-

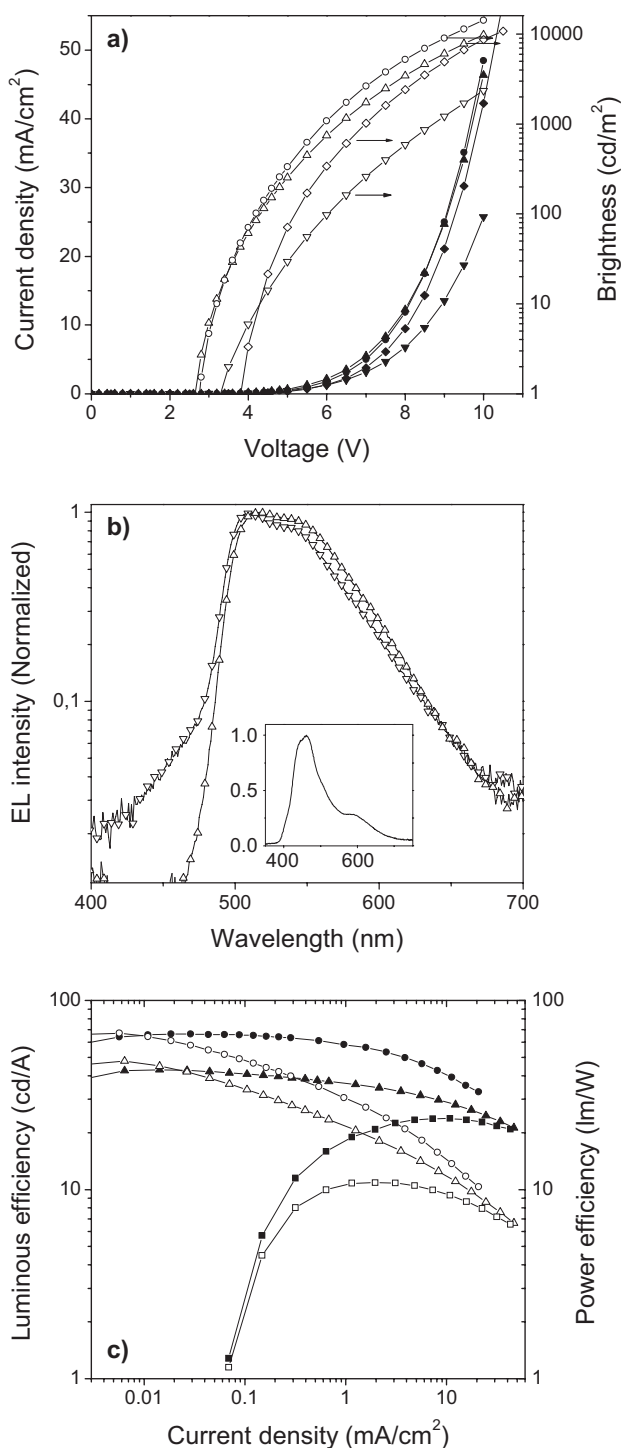


**Figure 2.** Performance of green-light-emitting electrophosphorescent devices. a)  $J$ - $V$  (solid symbols) and  $L$ - $V$  (open symbols) of several devices comprising the green-light-emitting dye  $\text{Ir}(\text{mppy})_3$  in a PVK:PBD matrix: G-X0-0.7 ( $\diamond$ ,  $\blacklozenge$ ), G-X1-0.7 ( $\nabla$ ,  $\blacktriangledown$ ), G-X1-6 ( $\triangle$ ,  $\blacktriangle$ ), and G-X2-6 ( $\circ$ ,  $\bullet$ ). b) Electroluminescence (EL) emission spectra of devices at  $20 \text{ mA cm}^{-2}$ : G-X1-0.7 and G-X1-6 (symbols as for (a)). The inset shows the EL spectrum of G-X1-0 (no dye added) at the same current density (axis labels as for main graph). c) Luminous efficiency (solid symbols) and power efficiency (PE; open symbols) of devices containing the green-light-emitting phosphor at a concentration of 6 wt% with a different layer structure: G-X0-6 ( $\square$ ,  $\blacksquare$ ), G-X1-6 ( $\triangle$ ,  $\blacktriangle$ ) and G-X2-6 ( $\circ$ ,  $\bullet$ ).

transporting layer (G-X1-0.7). Most noticeably, introduction of the HTL reduces the current density, even though the hole-injection barrier to the HOMO of the PVK matrix is considerably reduced in the multilayer device. We attribute the lower current in G-X1-0.7 mainly to the blocking of electrons (the reduction potential of the hole-transporting molecules can be estimated from the optical gap to be ca. 3.5 eV and the oxidation potential to be less than  $-3.2 \text{ V}$ ). Unfortunately, the efficiency of this simple multilayer device is quite disappointing, with rather low brightness at high current values. The electroluminescence (EL) spectrum (Fig. 2b) of G-X1-0.7 shows a distinct short-wavelength shoulder, which is not present in G-X0-0.7. To clarify the origin of this emission, we fabricated devices with the same composition of the charge-transporting PVK:PBD matrix, but without the emissive dopant (formally G-X1-0). In this case, a broad blue emission with low efficiency is observed (Fig. 2b, inset). Based on this result and similar observations on PVK:PBD:TPD blend layers,<sup>[18]</sup> we attribute this emission to an exciplex between the hole-transporting molecules in the HTL and the PBD contained in the emission layer.

On the other hand, this strong exciplex contribution and the reduction in device current upon insertion of the HTL indicate that a significant fraction of electrons are accumulated at the interface to the crosslinked layer. To ensure recombination of these electrons with holes on the phosphorescent dye, we raised the  $\text{Ir}(\text{mppy})_3$  concentration to 6 wt % (device G-X1-6). Consequently, the blue-light-emitting component in the EL emission spectrum vanished completely, resulting in pure-green-light emission, with the color coordinates  $x=0.33$ ,  $y=0.60$ . Concurrently, both the current density and the brightness increased significantly. We attribute this to the direct injection of holes from the HTL into the HOMO of  $\text{Ir}(\text{mppy})_3$ , followed by recombination with electrons accumulated at the interface between the HTL and the emission layer. Further evidence for this interpretation comes from the electrochemical data included in Figure 1, which can be regarded as a good measure of the energy levels.<sup>[27]</sup> Note, that the HOMO levels of both MUPD and OTPD almost align with that of  $\text{Ir}(\text{mppy})_3$ , but there is a 0.6 eV energy barrier for the hole injection to the HOMO level of PVK (Fig. 1). Moreover, at higher dye concentration ( $>5 \text{ wt } \%$ ), the dye molecules might form their own transport manifold within the PVK matrix, guiding holes deeper into the emission layer.

The luminous efficiency and PE for devices with identical emission-layer compositions are shown in Figure 2c. Compared to G-X0-6 (no HTL) the luminous efficiency in G-X1-6 is significantly larger (up to  $40 \text{ cd A}^{-1}$ ). Moreover, the efficiency maximum appears at rather low current values and drops only gradually with increasing current density. Concerning the driving voltage, the emission onset is significantly reduced compared to the devices with only PEDOT:PSS, resulting in a large PE of  $38 \text{ lm W}^{-1}$ . This suggests that the incorporation of the MUPD layer significantly improves hole injection, in addition to its role as the electron-blocking layer as discussed above.

To further increase the PE of the devices, we employed redox chemical doping of the HTL, which dramatically increases its conductivity and reduces the drive voltage in comparison with a nondoped reference device. Redox chemically doped carrier-transporting layers have been incorporated in OLEDs to build so-called “p-i-n structures” for improved carrier injection.<sup>[28–30]</sup> However, the doping of carrier-transporting layers leads to quenching of the EL close to the internal interface, which strongly reduces the EQE in thin devices (usually preferred due to their lower driving voltages and, thus, higher PE). Therefore, to avoid this, a second nondoped X-HTL was introduced. In such dual-injection-layer devices, the HOMO levels ideally should increase stepwise. Throughout this paper, we use a QUPD/OTPD combination, which has been found to be ideally suited. The optimized procedure will be described in detail elsewhere.<sup>[31]</sup> Introducing a second hole-injecting layer into the device (G-X2-6) affected the current only slightly, indicating that no additional energy barrier is formed for hole injection and transport. However, the light output was considerably enhanced (Fig. 2a).

In the G-X2-6 device, the luminous efficiency peaks at 67 cd A<sup>-1</sup>, corresponding an EQE of 18.8 % at a current density of 0.21 mA cm<sup>-2</sup>, a driving voltage of 4.4 V, and a brightness of 141 cd m<sup>-2</sup>. Given an out-coupling factor of 0.2 (assuming a refractive index of *n* = 1.8 for the polymer layer), the internal quantum efficiency of the device is approaching unity. The maximum PE (ca. 65 lm W<sup>-1</sup>) is at a current density of

0.01 mA cm<sup>-2</sup>. At a practical application brightness of 100 cd m<sup>-2</sup>, the PE is 50 lm W<sup>-1</sup>. Compared to the best polymer electrophosphorescent device reported in the literature, the EQE and PE are larger by a factor of about two (see Table 1). Moreover, the EQE of our green-light-emitting double X-HTL device well exceeds the value reported for the best device with Ir(ppy)<sub>3</sub> doped into the SM-CBP host (the chemical analogue of PVK)<sup>[5]</sup> and is only slightly smaller than the highest efficiency reported for SM devices.<sup>[6,30]</sup>

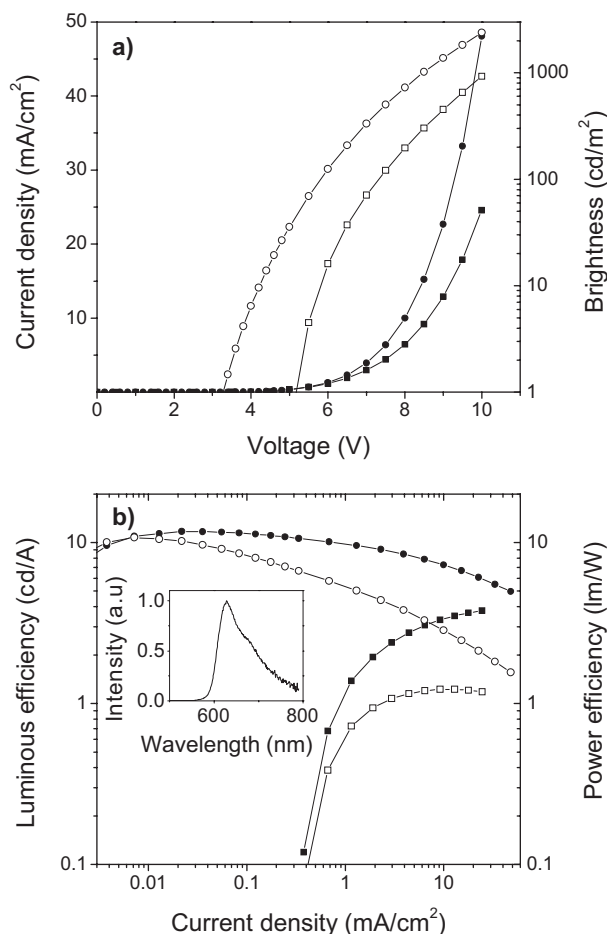
The concept developed for the green-light-emitting Ir(mppy)<sub>3</sub> phosphor worked equally well with the red-light-emitting bis(1-phenylisoquinoline)iridium(acetylacetonate) [Ir(piq)<sub>2</sub>(acac)]. SM devices with this dye co-evaporated with CBP yielded deep-red emission with an efficiency of 8.2 cd A<sup>-1</sup> (corresponding to 9.2 %).<sup>[8]</sup> Also note that the HOMO level of Ir(piq)<sub>2</sub>(acac) differs only slightly from that of Ir(mppy)<sub>3</sub>, suggesting that direct injection of holes from the cross-linked HTL should be as efficient as in the green-light-emitting devices.

Figure 3a shows the *J–L–V* characteristics of a red-light-emitting device with the structure R-X2-6, together with the *J–L–V* characteristics of the corresponding reference device R-X0-6. Similarly to the green-light-emitting devices, introducing the double-layer HTL structure significantly reduces the onset voltage, accompanied by a large increase in efficiency. As shown in Figure 3b, the improvement in luminous efficiency is most pronounced at low current levels, indicating

**Table 1.** Performance data of the best solution-processed multilayer devices as reported here. Also listed are the highest published values for red-, green- and blue-light-emitting polymer devices, the best small molecule devices with a CBP host (SM-CBP), and the best performance data for small molecule devices published up to now.

	Maximum luminous efficiency [cd A <sup>-1</sup> ]	Maximum EQE [%]	Maximum power efficiency [lm W <sup>-1</sup> ]	Performance @ 100 cd m <sup>-2</sup> [a]	Performance @ 1000 cd m <sup>-2</sup> [a]	Ref.
<b>red devices</b>						
this work	11.7	13	10.7	9.7 cd A <sup>-1</sup> 10.8 % 5.3 lm W <sup>-1</sup>	6.7 cd A <sup>-1</sup> 7.4 % 2.5 lm W <sup>-1</sup>	
best polymer SM-CBP matrix	11.0 n.a.	10.3 n.a.	n.a. n.a.	n.a. 10.3 % 8 lm W <sup>-1</sup>	n.a. n.a. n.a.	[20] [7]
SM other	6.9	n.a.	5.7	n.a.	n.a.	[36]
<b>green devices</b>						
this work	67.0	18.8	67	67 cd A <sup>-1</sup> 18.8 % 50.3 lm W <sup>-1</sup>	56 cd A <sup>-1</sup> 15.7 % 29.7 lm W <sup>-1</sup>	
best polymer SM-CBP matrix	n.a. 48.8	11.8 13.7	38.6 38.3	n.a. n.a.	n.a. n.a.	[21] [5]
SM other	n.a.	19.5	82	19.3 % 77 lm W <sup>-1</sup>	64 lm W <sup>-1</sup>	[30]
<b>blue devices</b>						
this work	11.5	5.7	4.9	11.5 cd A <sup>-1</sup> 5.7 % 4.9 lm W <sup>-1</sup>	9.3 cd A <sup>-1</sup> 4.6 % 2.7 lm W <sup>-1</sup>	
best polymer SM-CBP matrix	14 n.a.	n.a. 6.1	n.a. 7.7	n.a. n.a.	n.a. n.a.	[17] [34]
SM other	n.a.	14.4	11.9	n.a.	n.a.	[10]

[a] Luminous efficiency, EQE, power efficiency; n.a. = not available.



**Figure 3.** Performance of red-light-emitting electrophosphorescent devices. a)  $J$ - $V$  (solid symbols) and  $L$ - $V$  (open symbols) of devices comprising the red-emitting dye  $\text{Ir}(\text{pic})_2(\text{acac})$  in a PVK:PBD matrix: R-X0-6 ( $\square$ ,  $\blacksquare$ ) and R-X2-6 ( $\circ$ ,  $\bullet$ ). b) Luminous efficiency (solid symbols) and PE (open symbols) of the devices. Inset: Typical EL spectrum of all devices measured at  $20 \text{ mA cm}^{-2}$ .

balanced charge injection and a well-confined recombination zone. The peak luminous efficiency of the R-X2-6 device is  $11.7 \text{ cd A}^{-1}$ , corresponding to an EQE of 13 %, while the PE is  $10.7 \text{ lm W}^{-1}$  (for further details see Table 1). The inset of Figure 3b shows the EL spectrum of the devices ( $\lambda_{\text{max}} = 628 \text{ nm}$ ). The emission was found to be independent of driving conditions.

Finally, we attempted to apply the concept to blue-light-emitting electrophosphorescent LEDs using bis[(4,6-difluorophenyl)-pyridinato- $N,C^2$ ](picolinato) $\text{Ir}^{\text{III}}$  (FIrpic, see Fig. 1). However, several points are distinctly different when using FIrpic in combination with a PVK:PBD matrix, compared to the cases discussed above. Firstly, the HOMO level of FIrpic is now beyond that of PVK and, therefore, FIrpic molecules do not constitute hole traps within the PVK host matrix. Furthermore, recent time-resolved PL measurements suggest the existence of back-energy transfer from FIrpic to PBD due to the triplet energy of PBD being lower than that of FIrpic.<sup>[32]</sup> Consequently, we could not achieve efficient electrophos-

phorescence if FIrpic was added to a PBD-containing matrix. The emission properties could be drastically improved when using 1,3-bis[4-*tert*-butylphenyl]-1,3,4-oxadiazolyl]phenylene (OXD-7) as the electron-transporting species.

It has been shown previously that the efficiency of devices with PEDOT:PSS containing FIrpic in a PVK:OXD-7 matrix was maximum at a concentration of ca. 10–12 wt %.<sup>[12,14,17]</sup> For our devices of the structure B-X2, the efficiency increased monotonically with decreasing FIrpic concentration, with 5 wt % being the lowest concentration tested in this study. Figure 4 compares the  $J$ - $L$ - $V$  characteristics of devices B-X2-5 and B-X2-15 with a reference device of intermediate concentration (B-X0-10). As outlined above, introducing the bilayer X-HTL reduces the emission onset voltage significantly. Compared to the devices G-X2-6 and R-X2-6, the current density of the blue-light-emitting devices B-X2-5 at a given bias is significantly smaller, which is consistent with

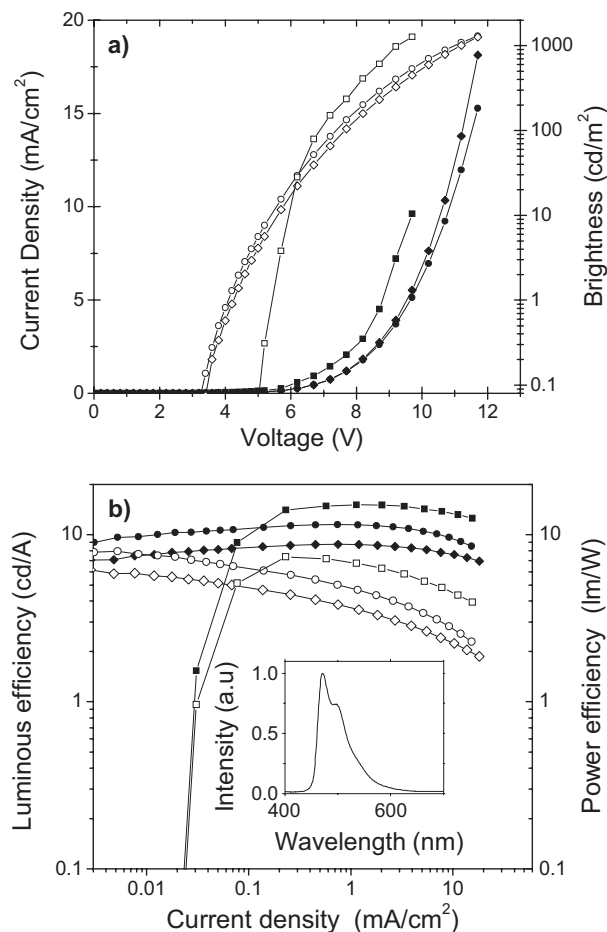


**Figure 4.** Performance of blue-light-emitting electrophosphorescent devices. a)  $J$ - $V$  (solid symbols) and  $L$ - $V$  (open symbols) of multilayer devices comprising the blue-light-emitting dye FIrpic in a PVK:OXD-7 matrix: B-X2-5 ( $\circ$ ,  $\bullet$ ) and B-X2-15 ( $\diamond$ ,  $\blacklozenge$ ). Also shown are the characteristics of a reference device with an intermediate dye concentration B-X0-10 ( $\square$ ,  $\blacksquare$ ). b) Luminous efficiency (solid symbols) and PE (open symbols) of the devices (shapes as for devices in (a)). Inset: Typical EL spectrum of all devices measured at  $20 \text{ mA cm}^{-2}$ .

the interpretation given above that direct transfer of holes from the X-HTL layer to the HOMO of Ir(mppy)<sub>3</sub> or Ir(piq)<sub>2</sub>(acac) contributes significantly to the injection and recombination of charges. Despite these differences, the general performance (onset voltage, peak efficiency at low current densities) of our blue-light-emitting multilayer devices is quite comparable to that of the corresponding green- or red-light-emitting device. However, the overall efficiency of the blue-light-emitting X-HTL devices is, surprisingly, lower compared with that of the corresponding B-X0-10 reference diode: the peak efficiency of the most efficient device B-X2-5 is 11.5 cd A<sup>-1</sup>, corresponding to an EQE of 5.7%, while the reference device B-X0-10 has a maximum efficiency of 12–16 cd A<sup>-1</sup>. Interestingly, the efficiency of B-X2-5 devices compares quite nicely with the values reported for FIrpic doped into the small-molecule CBP host (Table 1).<sup>[33,34]</sup> It has been previously pointed out that the triplet excited states on FIrpic are not well confined in the CBP matrix.<sup>[33,34]</sup> Finally we note that the lifetimes of our devices are well below the values needed for practical applications. The exact reason for this rapid degradation, which is generally observed for devices with a PVK:PBD host, has not, as yet, been identified.

In conclusion, we have demonstrated highly efficient multilayer polymer electrophosphorescent devices, which can be completely solution-processed for all three primary colors. In particular, we show that the EQEs of green- and red-light-emitting polymer electrophosphorescent devices are comparable to the best values reported in multilayer SM electrophosphorescent devices.<sup>[6,30,7,8]</sup> This is the first report of polymer electrophosphorescent devices with internal quantum efficiencies approaching unity, indicating that highly efficient electrophosphorescence is not a unique property of SM multilayer devices.

We show that the X-HTL concept is in principle suitable to increase the PE of blue-light-emitting electrophosphorescent devices as well, but that the EQE of these devices is not yet satisfactory. We attribute this to the deep HOMO position of the chosen phosphor, making the direct injection of holes onto the dye inefficient, as well as to a weak confinement of the triplet excited state on FIrpic. Thus, the optimization of 1) the HOMO position of the blue-light-emitting phosphor, 2) the triplet energy of the host, and 3) the HOMO level and triplet energy of the hole-transporting molecules in the X-HTLs is expected to improve the efficiency of blue-light-emitting polymer electrophosphorescent devices considerably.

We point out that our results were realized without incorporation of an exciton-blocking layer and an electron-transporting layer between the emission layer and the metallic cathode; insertion of these layers is often reported to be crucial to achieve high efficiencies in SM multilayer devices. Also, note that the overall thickness of our devices is higher than usual and we expect further improvements of the PE with optimized layer thickness. Further, no special efforts were made to improve the out-coupling efficiency.

## Experimental

Ir(mppy)<sub>3</sub>, Ir(piq)<sub>2</sub>(acac) and FIrpic were purchased from American Dye Sources and used as received. PBD and OXD-7 were purchased from Sensient and used as received.

PEDOT:PSS (Baytron P purchased from H. C. Starck) was spin-coated onto pre-cleaned and O<sub>2</sub>-plasma-treated indium tin oxide (ITO) substrates, yielding layers with a thickness of ca. 40 nm. The PEDOT:PSS layers were baked at 110 °C for half an hour to remove residual water.

In the X1 devices, the crosslinkable hole conductors (MUPD or OTPD synthesized according to [23]) were dissolved in THF, 0.5 wt % of the photoinitiator 4-octyloxydiphenyliodonium-hexafluoroantimonate (purchased from Aldrich) was added, and finally the solution was spin-cast atop the PEDOT:PSS layer to yield 20 nm thick films. The films were irradiated with light (365 nm wavelength) for 10 s and finally cured at 120 °C for one minute to promote crosslinking. This procedure yielded layers that were insoluble in all common organic solvents, which was verified by rinsing the films with good solvent and comparing the absorbance before and after the rinse. Under the conditions chosen here, we did not observe any difference, i.e., the films were fully crosslinked. In the X2 devices, redox chemical doping of the first layer was achieved by adding 2 wt % NO<sup>+</sup>SbF<sub>6</sub><sup>-</sup> (Aldrich), which stoichiometrically oxidizes the hole conductor. The second layer was deposited as described above.

A blend of PVK, PBD or OXD-7 (weight ratio 79:29), and the emitter (see Fig. 1) in chlorobenzene solution was spin-coated on top of the PEDOT:PSS and X-HTL films, yielding 70 nm thick films. Then, the samples were annealed at 80 °C for 30 min. The cathode, consisting of an ultrathin CsF interfacial layer with a nominal thickness of 1 nm and a ca. 70 nm thick Al layer, was deposited by thermal evaporation at a base pressure of 10<sup>-6</sup> mbar (1 mbar = 100 Pa).

All in all, the device thicknesses were 70, 90, or 110 nm for devices X0, X1, and X2, respectively.

Current-density–voltage characteristics were measured with a Keithley 2400 source measure unit. The brightness of the devices was recorded with a Minolta CS-100A camera. EL spectra of the devices were measured using a charge-coupled device fiber spectrometer (Ocean Optics). With the exception of the deposition of the PEDOT:PSS layer, all processes were carried out in a dry nitrogen atmosphere. The luminous efficiencies were converted to external quantum efficiencies and power efficiencies assuming Lambertian emission.

Received: September 5, 2005

Final version: December 6, 2005

Published online: March 17, 2006

- [1] C. W. Tang, S. A. Vanslyke, *Appl. Phys. Lett.* **1987**, *51*, 913.
- [2] J. H. Burroughes, D. D. C. Bradley, A. R. Brown, R. N. Marks, K. Mackay, R. H. Friend, P. L. Burns, A. B. Holmes, *Nature* **1990**, *347*, 539.
- [3] M. A. Baldo, D. F. O'Brien, Y. You, A. Shoustikov, S. Sibley, M. E. Thompson, S. R. Forrest, *Nature* **1998**, *395*, 151.
- [4] M. A. Baldo, S. Lamansky, P. E. Burrows, M. E. Thompson, S. R. Forrest, *Appl. Phys. Lett.* **1999**, *75*, 4.
- [5] T. Tsutsui, M. J. Yang, M. Yahiro, K. Nakamura, T. Watanabe, T. Tsuji, Y. Fukuda, T. Wakimoto, S. Miyaguchi, *Jpn. J. Appl. Phys., Part 2* **1999**, *38*, L1502.
- [6] C. Adachi, M. A. Baldo, M. E. Thompson, S. R. Forrest, *J. Appl. Phys.* **2001**, *90*, 5048.
- [7] A. Tsuboyama, H. Iwawaki, M. Furugori, T. Mukaide, J. Kamatani, S. Igawa, T. Moriyama, S. Miura, T. Takiguchi, S. Okada, M. Hoshino, K. Ueno, *J. Am. Chem. Soc.* **2003**, *125*, 12971.
- [8] Y. J. Su, H. L. Huang, C. L. Li, C. H. Chien, Y. T. Tao, P. T. Chou, S. Datta, R. S. Liu, *Adv. Mater.* **2003**, *15*, 884.
- [9] R. J. Holmes, B. W. D'Andrade, S. R. Forrest, X. Ren, J. Li, M. E. Thompson, *Appl. Phys. Lett.* **2003**, *83*, 3818.

- [10] S. J. Yeh, M. F. Wu, C. T. Chen, Y. H. Song, Y. Chi, M. H. Ho, S. F. Hsu, C. H. Chen, *Adv. Mater.* **2005**, *17*, 285.
- [11] M. J. Yang, T. Tsutsui, *Jpn. J. Appl. Phys., Part 2* **2000**, *39*, L828.
- [12] Y. Kawamura, S. Yanagida, S. R. Forrest, *J. Appl. Phys.* **2002**, *92*, 87.
- [13] W. G. Zhu, Y. Q. Mo, M. Yuan, W. Yang, Y. Cao, *Appl. Phys. Lett.* **2002**, *80*, 2045.
- [14] I. Tanaka, M. Suzuki, S. Tokito, *Jpn. J. Appl. Phys., Part 1* **2003**, *42*, 2737.
- [15] K. M. Vaeth, J. Diccillo, *J. Polym. Sci. Part B* **2003**, *41*, 2715.
- [16] X. H. Yang, D. Neher, D. Hertel, T. K. Däubler, *Adv. Mater.* **2004**, *16*, 161.
- [17] A. Nakamura, T. Tada, M. Mizukami, S. Yagyu, *Appl. Phys. Lett.* **2004**, *84*, 130.
- [18] X. H. Yang, D. Neher, *Appl. Phys. Lett.* **2004**, *84*, 2476.
- [19] A. van Dijken, J. Bastiaansen, N. M. M. Kiggen, B. M. W. Langeveld, C. Rothe, A. Monkman, I. Bach, P. Stossel, K. Brunner, *J. Am. Chem. Soc.* **2004**, *126*, 7718.
- [20] F. I. Wu, H. J. Su, C. F. Shu, L. Y. Luo, W. G. Diao, C. H. Cheng, J. P. Duan, G. H. Lee, *J. Mater. Chem.* **2005**, *15*, 1035.
- [21] M. Suzuki, S. Tokito, F. Sato, T. Igarashi, K. Kondo, T. Koyama, T. Yamaguchi, *Appl. Phys. Lett.* **2005**, *86*, 103507.
- [22] S. C. Lo, N. A. H. Male, J. P. J. Markham, E. B. Namdas, I. D. W. Samuel, P. L. Burn, *Adv. Mater.* **2002**, *14*, 975.
- [23] C. D. Müller, T. Braig, H. G. Nothofer, M. Arnoldi, M. Gross, U. Scherf, O. Nugken, K. Meerholz, *ChemPhysChem* **2000**, *1*, 207.
- [24] C. D. Müller, A. Falcou, N. Reckefuss, M. Rojahn, V. Wiederhirm, P. Rudati, H. Frohne, O. Nuyken, H. Becker, K. Meerholz, *Nature* **2003**, *421*, 829.
- [25] H. Yan, Q. Huang, B. J. Scott, T. J. Marks, *Appl. Phys. Lett.* **2004**, *84*, 3873.
- [26] X. Z. Jiang, A. K. Y. Jen, B. Carlson, L. R. Dalton, *Appl. Phys. Lett.* **2002**, *81*, 3125.
- [27] B. W. D'Andrade, S. Datta, S. R. Forrest, P. Djurovich, E. Polikarpov, M. E. Thompson, *Org. Electron.* **2005**, *6*, 11.
- [28] J. S. Huang, M. Pfeiffer, A. Werner, J. Blochwitz, K. Leo, S. Y. Liu, *Appl. Phys. Lett.* **2002**, *80*, 139.
- [29] M. Pfeiffer, S. R. Forrest, K. Leo, M. E. Thompson, *Adv. Mater.* **2002**, *14*, 1633.
- [30] G. F. He, M. Pfeiffer, K. Leo, M. Hofmann, J. Birnstock, R. Pudzich, J. Salbeck, *Appl. Phys. Lett.* **2004**, *85*, 3911.
- [31] C. D. Müller, K. Meerholz, unpublished.
- [32] X. H. Yang, F. Jaiser, S. Klinger, D. Neher, *Appl. Phys. Lett.* **2006**, *88*, 021107.
- [33] C. Adachi, R. C. Kwong, P. Djurovich, V. Adamovich, M. A. Baldo, M. E. Thompson, S. R. Forrest, *Appl. Phys. Lett.* **2001**, *79*, 2082.
- [34] R. J. Holmes, S. R. Forrest, Y. J. Tung, R. C. Kwong, J. J. Brown, S. Garon, M. E. Thompson, *Appl. Phys. Lett.* **2003**, *82*, 2422.